Phys. Status Solidi B **250,** No. 8, 1492–1495 (2013) / **DOI** 10.1002/pssb.201200977

physica status solidi b
www.pss-b.com
basic solid state physics

In silico tensile tests and design of hierarchical graphene fibres and composites

Federico Bosia[*,1] **and Nicola M. Pugno**[**,2,3]

[1] Department of Physics and "Nanostructured Interfaces and Surfaces" Centre of Excellence, University of Torino, Via P. Giuria 1, 10125 Torino, Italy
[2] Laboratory of Bio-Inspired & Graphene Nanomechanics, Department of Civil, Environmental and Mechanical Engineering, University of Trento, via Mesiano 77, 38123 Trento, Italy
[3] Center for Materials and Microsystems, Fondazione Bruno Kessler, Via Sommarive 18, 38123 Povo (Trento), Italy

Received 14 December 2012, revised 19 June 2013, accepted 21 June 2013
Published online 24 July 2013

Keywords graphene, hierarchy, mechanical properties, simulations

* federico.bosia@unito.it, Phone: +39 011 6707889, Fax: +39 011 6707020
** Corresponding author: nicola.pugno@unitn.it, Phone: +39 0461 282525, Fax: +39 0461 282599

In this contribution, we apply a hierarchical fibre bundle model (HFBM), previously developed to estimate the mechanical properties of multiscale carbon nanotube (CNT)-based structures, to the case of graphene macroscopic cables. The nonlinear elastic properties of graphene and its exceptional intrinsic strength, with mean Young's modulus of 1 TPa, third-order elastic stiffness of −2.0 TPa and intrinsic strength of 130 GPa, are drawn from recent experimental studies. The model allows to derive macroscopic characteristics like strength, stiffness, toughness as a function of hierarchical structure, starting from statistically distributed properties at the nanoscale and without the introduction of additional *ad hoc* parameters. The influence of the presence of defects in the graphene bundles is evaluated. We also analyse the properties of graphene-reinforced composites, including the influence of the volume fraction of a ductile polymeric matrix. We show that the composite properties can be engineered to optimize strength and/or stiffness, and that the present model can be a useful tool to help pursue this objective

1 Introduction In recent years, much effort has gone into investigating graphene for its exceptional electronic, thermal, optical and mechanical properties. Various different graphene nano/micro-structures have by now been synthesized and characterized, including graphene paper [1], graphene nanoribbons [2] and also macroscopic assembled graphene fibres [3]. In addition, large area growth techniques have been increasingly developed thanks to specific research in this direction [4, 5]. Another important field is that of graphene-based composites, which could provide the means to harness graphene's exceptional properties for applications [6].

From a mechanical point of view, graphene can be considered 'the strongest material ever measured', ever since Lee et al. managed to measure the elastic properties and intrinsic breaking strength of free-standing monolayer graphene membranes by nanoindentation in an atomic force microscope [7]. In this study, graphene was found to display a nonlinear elastic behaviour of the type

$$\sigma = E\varepsilon + D\varepsilon^2, \tag{1}$$

where σ is the stress, ε the strain, $E = (1.0 \pm 0.1)$ TPa and $D = (-2.0 \pm 0.4)$ TPa. Moreover, its measured intrinsic strength was $\sigma_f = (130 \pm 10)$ GPa, which is the highest value found for any material in nature [7]. However, it is unclear what the effect of defects, grain boundaries, etc. could have on these values. In carbon nanotubes (CNTs), a low-dimensional material like graphene, the introduction of a single vacancy can determine a drop in strength of up to 20% [8]. CNT-based composites have been widely studied in past years [9]. Although graphene can be considered as a two-dimensional system, as opposed to CNTs that are usually considered one-dimensional, both share high aspect ratios and exceptional mechanical properties, which can be exploited in composites. Thus, another question is: in graphene composites, how can we optimize mechanical performance (stiffness, strength, toughness…) by varying constituent material properties, mixing ratio, hierarchical structure or other parameters? Clearly, experimental investigations to reply to these questions would entail very cumbersome studies, therefore it is convenient to develop numerical

models to predict mechanical multiscale behaviour of graphene structures and composites. To do this, we have adopted a very simple modelling approach, previously used to perform multiscale simulations on the stiffness and strength of defective nanotube-based mega-structures [10], or for the design of supertough nanofibers inspired by spider silk [11], where CNT-polyvinyl alcohol (PVA) composites were analysed. The model is presented in Section 2 and simulation results on graphene ribbons and composites are presented in Section 3.

2 Hierarchical fibre bundle model (HFBM) The model used here is related to that proposed by the authors in the past [10, 12], which is based on a fibre bundle model (FBM) approach, and whereby a specimen is discretized in an array of springs (or 'fibres') arranged in series and parallel. The individual fibres have randomly assigned statistically distributed strengths, in this case according to the two-parameter Weibull distribution, which is described by the following equation [13]:

$$p(\sigma) = \frac{m}{\sigma_0}\left(\frac{\sigma}{\sigma_0}\right)^{m-1} e^{-(\sigma/\sigma_0)^m}, \qquad (2)$$

where σ_0 and m are the scale and shape parameters, respectively. In order to model heterogeneous media, such as in composites, the fibres of each bundle can assume different mechanical properties. The k-th fibre type is characterized by a Young's modulus E_k, length l_k, cross-sectional area A_k and Weibull-distributed fracture strengths, the latter characterized by a scale parameter σ_{0k} and shape parameter m_k. The various types of fibres combine in forming 'bundles', with complex mechanical behaviour emerging from the mechanical properties and arrangement of the constituent fibres. The specimen's stress-strain behaviour is determined by imposing an increasing displacement and 'rupturing' individual fibres in the bundle (*i.e.*, setting their stiffness to zero) when their statistically assigned strength is exceeded. After each fracture event, the load is redistributed uniformly among the fibres in the same bundle as the fractured one (equal load sharing). The bundle strength is obtained as the maximum stress value reached in the simulation before failure, *i.e.*, when all parallel fibres of the bundle have failed. Since the fibre strengths are assigned randomly according to the Weibull distribution, results differ for each simulation, and average trends can be derived from repeated simulations.

The model is replicated in a hierarchical scheme at various length scales ('levels') to predict the multiscale mechanical behaviour. This is implemented as described in Ref. [10], *i.e.*, the input mechanical behaviour of a level $i = h - 1$ 'fibre' or subvolume is statistically inferred from the average output deriving from repeated level h simulations, that of a level $i = h - 2$ subvolume from level $i = h - 1$ simulations and so on, down to the lowest hierarchical level $i = 1$. Overall, the specimen is modelled as an ensemble of N_1 subvolumes arranged in a bundle. Each of these subvolumes is in turn constituted by N_2 subvolumes, arranged in a bundle as before. This scheme is applied for h 'generations', up to a level h subvolume, which is constituted N_a type 'a' fibres, N_b type 'b' fibres and so on. This is schematically shown in Fig. 1.

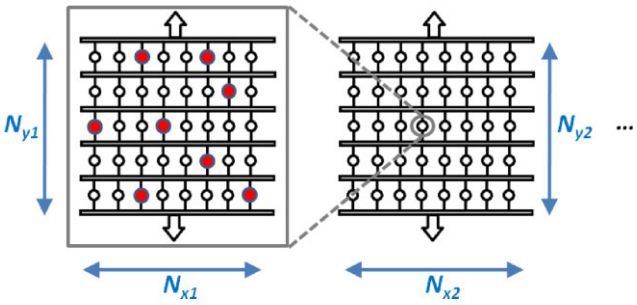

Figure 1 Schematical representation of hierarchical scheme used in the HFBM model.

3 Simulation results Two specific systems are considered in the following, namely graphene ribbon bundles/fibres and graphene-reinforced polymer composites.

3.1 Graphene ribbons/fibres Graphene nanoribbons can be obtained through various methods: unzipping of CNTs [2], STM lithography, catalytic hydrogenation, using thermally activated Ni nanoparticles, exfoliation of chemically modified and expanded graphite [14]. We wish to numerically characterize the uniaxial tensile mechanical behaviour of nanoribbon bundles and evaluate the possible influence of defects on the overall response at microscale and macroscale. In order to do this, we use the previously mentioned parameters derived experimentally by Lee et al. [7] for single graphene flakes/ribbons at level 1 of our HFBM. These material parameters were obtained through nanoindentation experiments, but are applicable to uniaxial tensile tests. To use these data to construct the desired Weibull distribution in Eq. (2), we assume that each material parameter is normally distributed around the given mean value, with standard deviation equal to its uncertainty. We then fit the resulting normal distribution with a Weibull distribution, and use the corresponding Weibull shape and scale parameters as inputs of the level 1 hierarchical simulations. An example is shown in Fig. 2 for the Weibull distribution for the strength of the graphene ribbons in the bundle, corresponding to scale and shape parameters of $\sigma_0 = 131$ GPa and $m = 14$. As can be seen, the discrepancy between the normal and Wiebull distributions is small. The specimens are discretized with $N_x = 10^3$ and $N_y = 10^2$ fibres. This choice of parameters provides a sufficiently refined discretization of the specimen so as to guarantee that simulation results are independent of the 'grid'. Simulations are repeated 10^3 times to calculate mean values.

Some typical output stress–strain curves for the graphene ribbon bundles are shown in Fig. 3. The different curves correspond to separate runs, which differ due to the statistical variation in level 1 parameters. The nonlinear elastic constitutive law from Ref. [1] is reflected in the

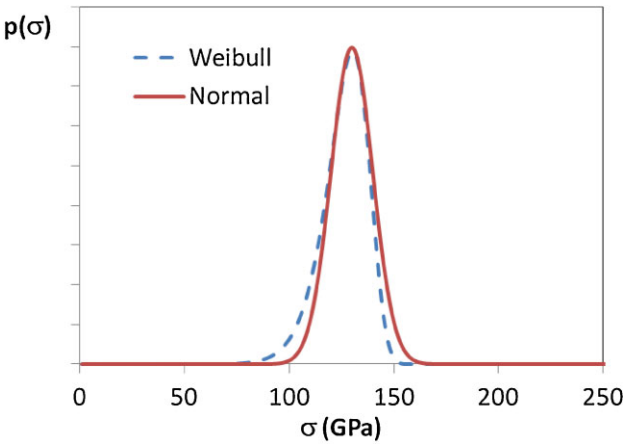

Figure 2 Normal strength distribution for single graphene ribbons derived from Ref. [7] and corresponding fitted Weibull distribution.

observed nonlinear behaviour up to fracture. The obtained mean bundle strength is 91 GPa, showing how 'upscaling' leads to a considerable strength decrease, even in the absence of defects. This is due to the statistical variation in the ribbon strengths in the bundle, so that their failure is not simultaneous, and the maximum stress value in simulations is reached only for a given percentage of surviving ribbons, giving a reduced strength value.

In addition to this effect, the role of defects (such as single or multiple vacancies, carbon adatoms, substitutional impurities [15]) is decisive in determining the overall strength of a graphene ribbon bundle. This can be verified by introducing randomly distributed 'voids' in the array of fibres at single level in the model, with a set volume ratio (*i.e.*, percentage). As expected, given the low-dimensionality of graphene, the presence of even small percentages of defects in the graphene ribbon bundles reduces the strength dramatically. Results are shown in Fig. 4 in log scale: a 100-fold strength reduction is obtained for a defect percentage of approximately 10%.

To compare these predictions with experimental values, we consider the data from Xu and Gao [3] on graphene

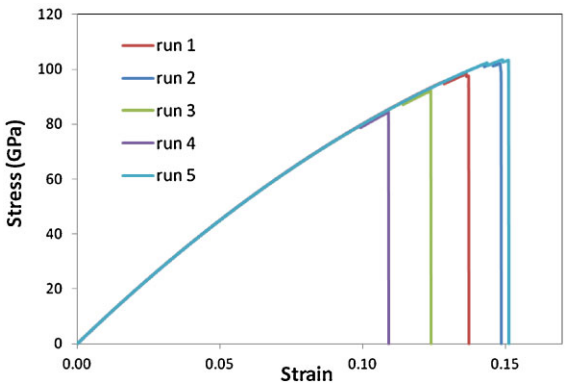

Figure 3 Simulated stress–strain curves for a graphene ribbon bundle in repeated runs.

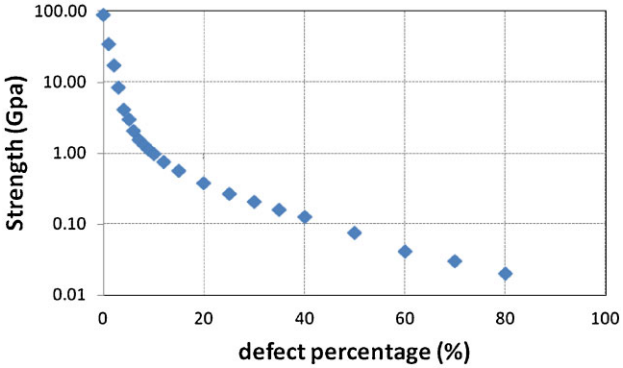

Figure 4 Strength decrease as a function of defect percentage.

fibres. The fibre dimensions are length $l = 1$ m and radius $r = 20$ μm. Experimental results for tensile tests on these fibres yield strength values of approximately 140 MPa. In simulations, since it is necessary to span from the length dimensions of graphene flakes (10^{-6} m), for which mechanical properties are known, to the length of full fibres (10^{0} m), the number of hierarchical levels h necessary to model the chosen system in multiscale simulations and the (N_x, N_y) discretization at each hierarchical level need to be chosen so that $(N_x)^h = 10^6$. For simplicity, we choose a constant discretization at each level of $N_x = N_y = 100$, which provides a sufficiently refined grid, and $h = 3$.

Simulations are carried out for various defect percentages (uniformly distributed at all levels). In this case, we are essentially considering single-vacancy defects, modelled as missing 'links' (fibres) in the lattice. An agreement with experimental values is obtained for a defect percentage of approximately 20%. Thus, it is possible to infer the actual defect percentage of the material, based on the measured mechanical properties, through numerical modelling. This result of a very high defect content is in keeping with the analysis in Ref. [3] whereby the 'mechanical properties of the fibres can be greatly improved by optimization of the spinning process and post-annealing to decrease the voids'. Numerical results for the determined defect percentage of 20% are reported in Fig. 5, and show a power law-type

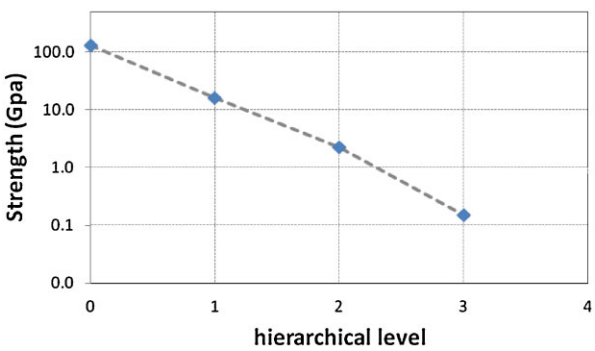

Figure 5 Strength decrease for a graphene fibre as a function of hierarchical level for a defect percentage of 20%.

decrease in the predicted strength with increasing hierarchical level, and therefore size.

3.2 Graphene–polyvinyl chloride (PVC) composites The second graphene-based system we consider is a graphene-reinforced PVC composite. Experimental data exist in the literature on this system which is of interest due to its flexibility, conductivity, high mechanical strength and thermal stability [16]. In particular, researchers found that a significant enhancement in the mechanical properties of pure PVC films was obtained with a 2 wt.% loading of graphene, such as a 58% increase in Young's modulus and an almost 130% improvement of tensile strength. HFBM simulations have been carried out on this system using for PVC a tensile strength of 25 MPa and Young's modulus of 0.8 GPa [16], and considering increasing weight percentages of graphene fibres. Again, three hierarchical levels and $N_x = N_y = 100$ at each level are used for the simulations. In this case, at the first hierarchical level, corresponding to the 1–100 μm range, a composite structure is considered, composed by two types of fibres in varying weight percentages. The Young's modulus and strength distributions of graphene are those mentioned in Section 3.1, while those for PVC are derived in a similar manner from the corresponding mean values, with slightly wider Weibull distributions ($m = 3$) to account for a greater variability in the matrix properties. Simulations at levels 2 and 3 are carried out for 'homogeneized' samples, with a single fibre type whose properties are derived from level 1 simulations.

Numerical results are compared to experimental data in Fig. 6, and very good agreement is found. A linear increase in Young's modulus is found for increasing weight fractions of graphene, at least for small percentages, which is in the range of values that can be realized experimentally. For greater weight fractions, experimental stiffness values are found to saturate, probably due to the fact that an imperfect dispersion of graphene is obtained in the polymeric matrix.

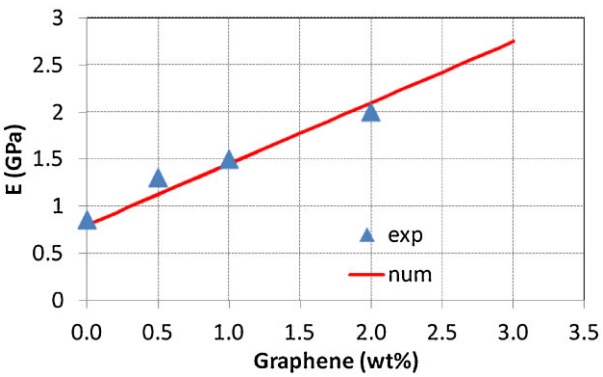

Figure 6 Stiffening effect for increasing graphene reinforcement weight concentrations in graphene–PVC composites (experimental data from Ref. [14]).

4 Conclusions Graphene shows great promise in the fields of mechanics and materials science due to its exceptional properties, and may prove a valid alternative to CNTs, for example as a reinforcement in composites. The presented HFBM model provides a simple but highly predictive tool to simulate the mechanical behaviour of nanostructured hierarchical graphene-based materials. In particular, the influence of defects at various hierarchical levels can be evaluated in macroscopic graphene fibres, and proves to be a critical parameter, with realistic estimates at about 20% for some recently produced fibres [3]. As far as graphene-polymer composites are concerned, the graphene reinforcement is shown to be very effective in the stiffening and strengthening of PVC-matrix composite materials. In future, the presented HFBM can be used to evaluate the potential performance of graphene composites and design tailor made characteristics for specific applications.

Acknowledgements This work is supported by the ERC Ideas Starting Grant no. 279985 'BIHSNAM—Bio-Inspired Hierarchical Super Nanomaterials'. Computational resources were provided by the Politecnico di Torino's DAUIN HPC Initiative (http://dauin-hpc.polito.it).

References

[1] H. Chen, M. B. Müller, K. J. Gilmore, G. G. Wallace, and D. Li, Adv. Mater. **20**(18), 3557–3561 (2008).
[2] D. V. Kosynkin, A. L. Higginbotham, A. Sinitskii, J. R. Lomeda, A. Dimiev, B. K. Price, and J. M. Tour, Nature **458**, 872–876 (2009).
[3] Z. Xu and C. Gao, Nature Commun. **2**, 571 (2011).
[4] X. Li, W. Cai, J. An, S. Kim, J. Nah, D. Yang, R. Piner, A. Velamakanni, I. Jung, E. Tutuc, S. K. Banerjee, L. Colombo, and R. S. Ruoff, Science **324**(5932), 1312–1314 (2009).
[5] S. Bae, H. Kim, Y. Lee, X. Xu, J. Park, Y. Zheng, J. Balakrishnan, T. Lei, H. R. Kim, Y. Il Song, Y.-J. Kim, K. S. Kim, B. Özyilmaz, J.-H. Ahn, B. H. Hong, and S. Iijima, Nature Nanotechnol. **5**, 574–578 (2010).
[6] S. Stankovich, D. A. Dikin, G. H. B. Dommett, K. M. Kohlhaas, E. J. Zimney, E. A. Stach, R. D. Piner, S. T. Nguyen, and R. S. Ruoff, Nature **442**, 282–286 (2006).
[7] C. Lee, X. Wei, J. W. Kysar, and J. Hone, Science **321**, 385–388 (2008).
[8] N. M. Pugno, Int. J. Fract. **140**, 158 (2006).
[9] A. S. Wu and T. W. Chou, Mater. Today **15**(7–8), 302–310 (2012).
[10] N. M. Pugno, F. Bosia, and A. Carpinteri, Small **4**(8), 1044–1052 (2008).
[11] F. Bosia, M. Buehler, and N. M. Pugno, Phys. Rev. E **82**, 056103 (2010).
[12] F. Bosia, N. M. Pugno, and A. Carpinteri, Int. J. Solids Struct. **45**, 5856–5866 (2008).
[13] W. Weibull, J. Appl. Mech. – Trans. ASME **18**, 293–297 (1951).
[14] F. Bonaccorso, A. Lombardo, T. Hasan, Z. Sun, L. Colombo, and A. Ferrari, Mater. Today **15**(12), 564–589 (2012).
[15] F. Banhart, J. Kotakoski, and A. V. Krasheninnikov, ACS Nano **5**(1), 26–41 (2011).
[16] S. Vadukumpully, J. Paul, N. Mahanta, and S. Valiyaveettil, Carbon **49**, 198–205 (2011).